



Article

Understanding the Entrainment Behavior of Gangue Minerals in Flake Graphite Flotation

Yangshuai Qiu ^{1,2}, Zhenfei Mao ¹, Kangkang Sun ^{3,*}, Lingyan Zhang ^{1,2}, Yupeng Qian ^{1,2}, Tao Lei ¹, Wenbo Liang ¹ and Yaxin An ¹

¹ School of Resources and Environmental Engineering, Wuhan University of Technology, Wuhan 430070, China

² Hubei Key Laboratory of Mineral Resources Processing & Environment, Wuhan 430070, China

³ School of Chemical Engineering, The University of Queensland, Brisbane, QLD 4072, Australia

* Correspondence: kangkang.sun@uq.edu.au

Abstract: Flotation is one of the most used methods to upgrade natural graphite resources. However, the efficiency is usually decreased due to the entrainment of undesirable fine gangue minerals. In this work, the impact of different factors such as particle size, pulp density, and flotation reagent on the entrainment of mica and quartz in a flake graphite flotation was studied. The single gangue mineral flotation results showed increased gangue entrainment when reducing the particle size of gangue minerals and increasing the pulp density. Moreover, the flotation of artificial mixtures indicated enhanced entrainment of mica and quartz in the presence of graphite particles. The collector and frother also strongly affect gangue entrainment by modifying the structure and stability of the froth. Kerosene, which has a prominent deforming feature, can reduce gangue entrainment more effectively than diesel.

Keywords: entrainment; froth flotation; quartz; mica; flake graphite



Citation: Qiu, Y.; Mao, Z.; Sun, K.; Zhang, L.; Qian, Y.; Lei, T.; Liang, W.; An, Y. Understanding the Entrainment Behavior of Gangue Minerals in Flake Graphite Flotation. *Minerals* **2022**, *12*, 1068. <https://doi.org/10.3390/min12091068>

Academic Editor: Kevin Galvin

Received: 6 July 2022

Accepted: 22 August 2022

Published: 24 August 2022

Publisher's Note: MDPI stays neutral with regard to jurisdictional claims in published maps and institutional affiliations.



Copyright: © 2022 by the authors. Licensee MDPI, Basel, Switzerland. This article is an open access article distributed under the terms and conditions of the Creative Commons Attribution (CC BY) license (<https://creativecommons.org/licenses/by/4.0/>).

1. Introduction

Graphite is a non-metallic mineral that has been versatile in various scientific and technological fields, including metallurgy, electronics, national defense, and aerospace [1,2]. Natural graphite is typically found in three commercial varieties: crystalline flake, microcrystalline or amorphous, and crystalline vein or lump [3]. Because of the natural hydrophobicity and floatability of graphite, froth flotation is one of the most prevalent and cost-effective methods for enriching graphite resources [4–6]. In flotation, hydrophobic graphite particles are preferentially collected by air bubbles and transported to the surface, leaving the hydrophilic gangue minerals in the suspensions and discharged as tailings [7]. However, the upgrading efficiency of flotation is usually limited, especially for fine flake [8,9] and amorphous graphite resources [10–13]. Generally, the finer the association between graphite and gangue minerals, the lower the grade of final flotation products [14–16]. The main reason is that besides true flotation, target minerals and gangue can also enter the concentrate product via entrainment and entrapment [17–20]. As illustrated in Figure 1, entrainment is an undesirable process in which mineral particles, even hydrophilic ones, are entrapped in the water phase between the liquid films and mechanically moved upward with the rising foam. Entrapment refers to the hydrophilic gangue mineral particles being sandwiched within the hydrophobic particles and transported into the mineral concentrate.

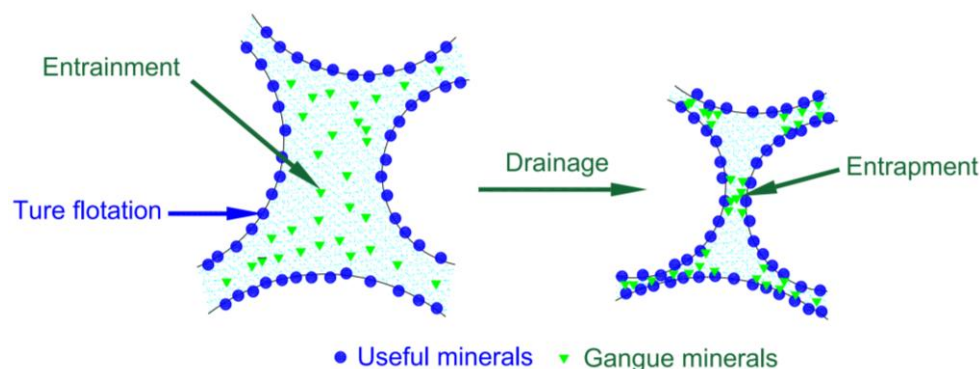


Figure 1. The schematical illustration of froth entrapment in the flotation process.

Compared to entrapment, gangue entrapment is more dominant when graphite and gangue particles are ground to a fine or ultra-fine size [20–22], significantly reducing the separation efficiency between graphite and fully liberated gangue in flotation. Such entrapment is also prevalent in many other ores, such as coal [23], ultra-fine sphalerite [24], Au/Cu sulfide ore [25], and base metal ores [26].

The entrapment behavior of hydrophilic gangue in mineral flotation has been studied for decades, and many factors contribute to entrapment, such as gangue properties [17,27], slurry viscosity, froth structure [28], particle mass [29], and shape [20,30]. However, few have focused on the impact of hydrophobic minerals on the entrapment behavior of gangue, despite their coexistence in the flotation pulp. Ata et al. [29] proposed that hydrophobic particles can substantially affect the froth structure, which in turn influences the drainage of hydrophilic particles from the froth. Moreover, our recent flotation study [31] has shown a considerably increased collection of gangue minerals, including mica and quartz, in the presence of graphite particles. We confirmed such phenomena as enhanced entrapment caused by the hydrophobic graphite particles. However, the underlying impact of particle hydrophobicity on gangue entrapment is still unclear.

Therefore, we intended to further explore the entrapment of these gangues and investigate the effect of several contributing factors, including particle size, pulp density, and flotation reagent, on gangue entrapment. As the main gangue in natural graphite ore, the hydrophilic mica and quartz were selected, and their entrapment behavior in the absence and presence of hydrophobic graphite minerals was studied via batch flotation tests. Water recovery of froth product, entrapment rate, and entrapment recovery were calculated and selected as the main parameters to evaluate the entrapment behavior.

2. Materials and Methods

2.1. Materials

The test samples, graphite and mica, were obtained from Hubei, China, and quartz was obtained from Jiangxi, China. All samples were first ground in a conical ball mill using zirconia ball as the grinding medium and then divided into different size fractions, including +150 μm , –150 to +74 μm , –74 to +45 μm , –45 to +38 μm , –38 to +30 μm , –30 to +20 μm , –20 to +10 μm , and –10 μm . Before testing, the mica and quartz samples were subjected to magnetic separation and acid treatment to remove magnetic impurities and other contaminants. X-ray diffraction (XRD) and X-ray fluorescence (XRF) analyses were used to determine the mineralogical and chemical composition of the samples, and the results are given in Figure 2 and Table 1, respectively. It should be noted that the fixed carbon (FC) content of the graphite sample was analyzed using the Chinese standard GB/T3521-2008, assaying 96.13 wt %. The particle size distributions of the samples, as demonstrated in Figure 3, were measured using a BT-9300S laser particle size analyzer. In addition, Figure 4 shows the SEM images of the samples (–74 μm size fraction). It can be seen that graphite (Figure 4a,b) and mica (Figure 4c,d) show a similar flaky shape, while quartz particles (Figure 4e,f) are mostly granular.

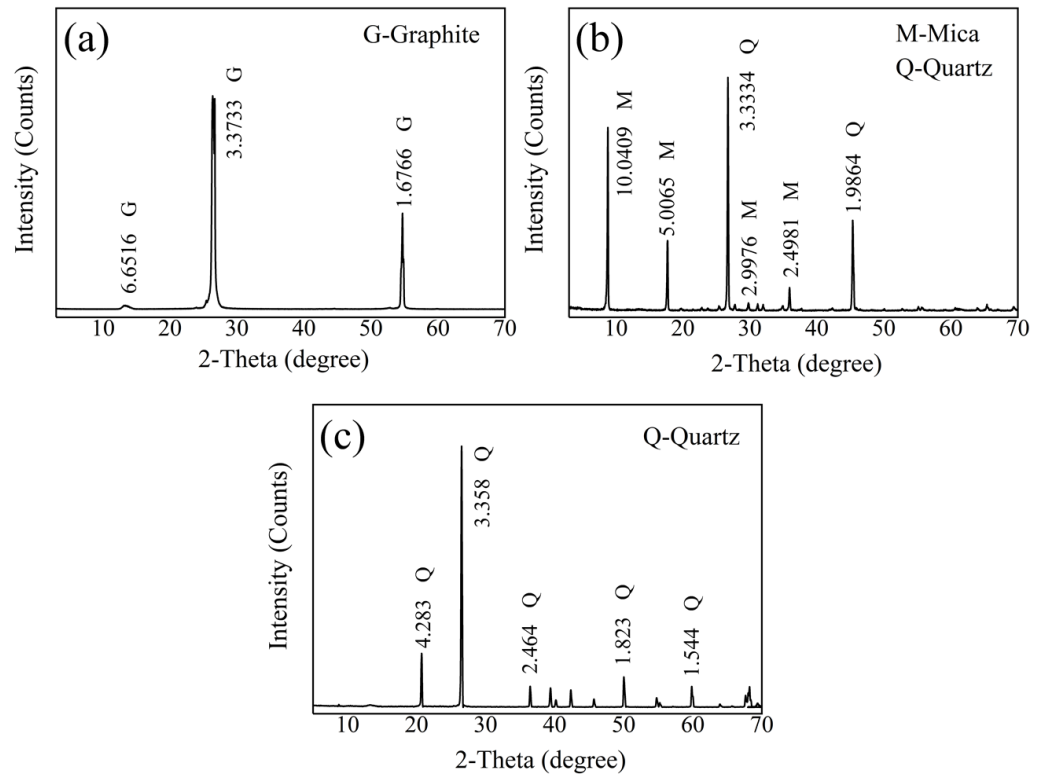


Figure 2. XRD spectra of the test samples: (a) graphite; (b) mica; and (c) quartz.

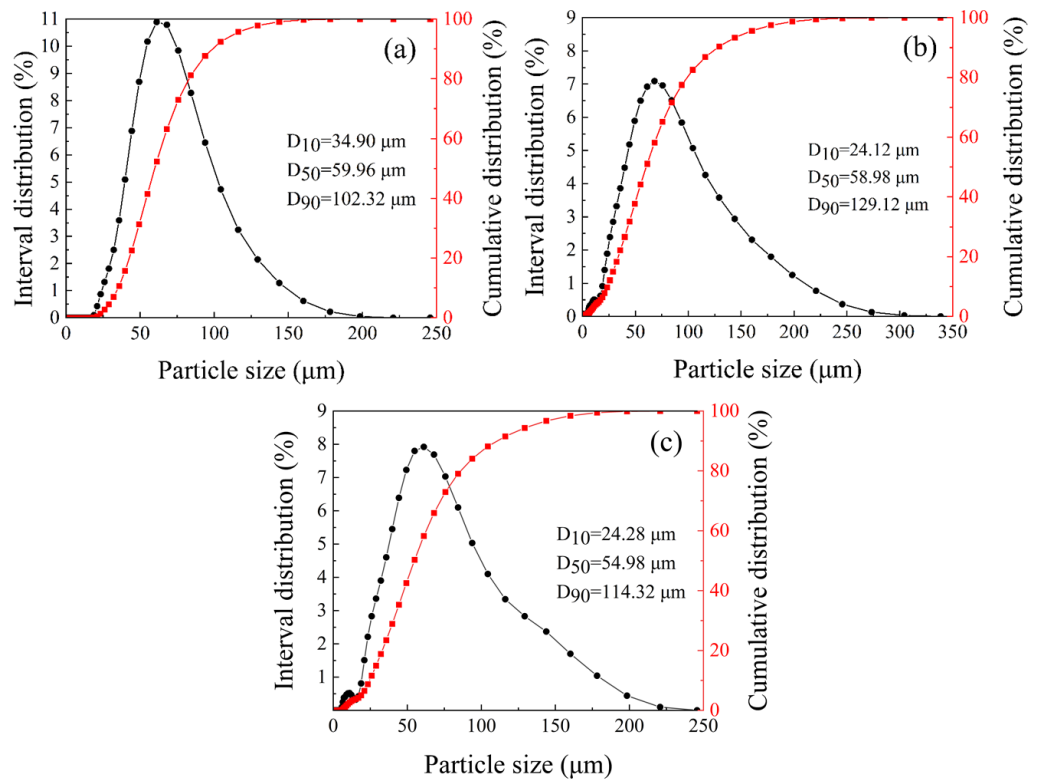
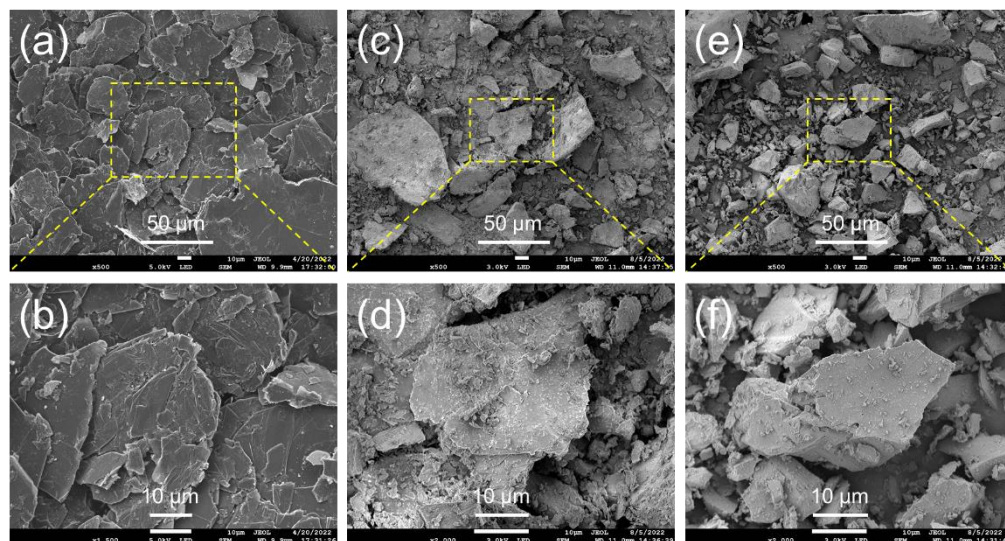


Figure 3. Particle size distribution of the test samples: (a) graphite; (b) mica; and (c) quartz.

Table 1. Chemical composition of the test samples (wt %).

Minerals	SiO ₂	Al ₂ O ₃	K ₂ O	Na ₂ O	Fe ₂ O ₃	SO ₃	CaO	FC	Other
Mica	48.51	37.04	9.17	1.09	0.48	0.09	0.05	/	3.57
Quartz	98.87	0.25	0.28	/	0.10	0.04	0.04	/	0.42
Graphite	1.78	0.64	0.16	0.09	0.57	/	/	96.13	0.63

**Figure 4.** SEM images of the test samples: (a,b) graphite; (c,d) mica; and (e,f) quartz.

The collector kerosene was purchased from Kermel Chemical Reagent Co., Ltd. (Kermel, Tianjin, China), and the frother terpenic oil, MIBC, and sec-octanol (C₈H₁₈O) were purchased from Aladdin Biochemical Technology Co., Ltd. (Shanghai, China). The surface tension of these frothers in solution was determined by the platinum ring method using a BZY-102 surface tension tester. All the chemicals were of analytical grade and used directly without further purification. Deionized water (resistivity of 18.25 MΩ·cm) was used in this work.

2.2. Flotation Tests

Batch flotation tests of single and mixed minerals were carried out using an RK/FGC5-35 flotation cell (140 mL). A schematic illustration of the flotation cell is shown in Figure 5. For single mineral flotation, 2 g of gangue mineral or graphite (denoted as M_g) was first stirred in 100 mL of water (lower than the maximum capacity of the flotation cell to avoid undesirable overflow during flotation) to prepare the flotation slurry before adding the desired collector and frother. The 3 min continuous agitation at 1600 rpm was applied at each step of the reagent addition followed by aeration (with a constant airflow rate of 60 cm³/min), flotation, and bubble scraping for another 3 min. All flotation tests were conducted at around pH 7. The flotation of mixed minerals was conducted following the same procedure but with a mixed feeding of 2 g graphite and 0.5 g gangue mineral, which are referred to as m_g and m_t , respectively. The water recovery, flotation recovery, and entrainment rate were calculated using Equations (1)–(3), respectively [17].

$$R_W = \frac{M_1 - M_2}{M_w} \times 100\% \quad (1)$$

$$R_M = \frac{M_2}{M_g} \times 100\% \quad (2)$$

$$e_g = \frac{R_M}{R_W} \quad (3)$$

where R_W is the water recovery in the froth product, %; R_M is the flotation recovery of gangue by entrainment, %; e_g is the degree of entrainment; M_w is the weight of water consumed during flotation, g; M_1 and M_2 are the wet and dry weights of the froth product, respectively, g; and M_g is the weight of the feed mineral, g.

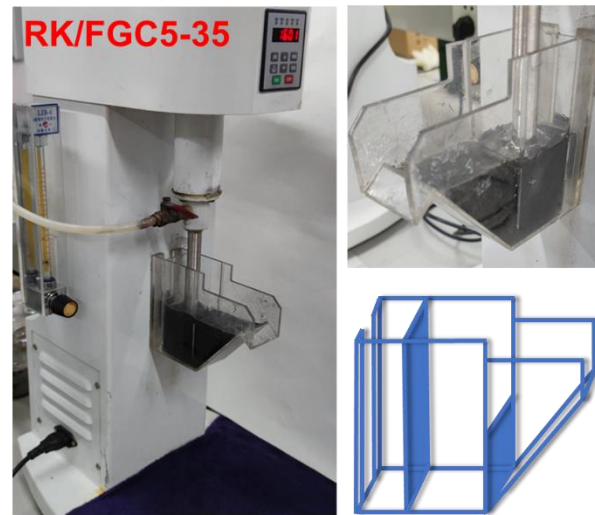


Figure 5. The schematical illustration of the RK/FGC5-35 flotation cell.

In mixed flotation, the flotation recoveries of graphite and gangue minerals were calculated by Equations (4) and (5) [32].

$$R_m = \left[1 - \frac{m_2 - m_1 A_g}{m_t (A_m - A_g)} \right] \times 100\% \quad (4)$$

$$R_g = \left[1 - \frac{m_1 A_m - m_2}{m_g (A_m - A_g)} \right] \times 100\% \quad (5)$$

where R_m and R_g are the recoveries of gangue and graphite minerals in froth product, respectively, %; m_1 and m_2 are the total mass and ash mass of the non-floated product, g; m_t and m_g are the weight of gangue and graphite minerals, respectively, g; A_m and A_g are the ash content of gangue and graphite minerals, respectively, %.

3. Results and Discussion

3.1. The Entrainment Behavior of Single Gangue Mineral Flotation

3.1.1. Particle Size

Particle size is one of the most important factors affecting gangue entrainment. Therefore, the entrainment behavior of mica and quartz gangue minerals with different size fractions were investigated, and the results are shown in Figure 6. Only frother sec-octanol was added during the flotation test. Note that despite the fixed frother feeding, the different surface areas among particles with various size fractions might result in ambiguous surfactant adsorption density, making the interpretation of particle size on entrainment dubious. Nevertheless, such an impact should be relatively negligible given that only a small amount of frother was added to modify the froth properties. It is noteworthy in Figure 6a that the water recovery in froth (R_W) significantly increases as the gangue particle size decreases. The R_W for mica and quartz with a particle size of +150 μm was 5.78% and 3.61%, respectively, while that with a particle size of −10 μm significantly increased to 22.34% and 17.22%, respectively.

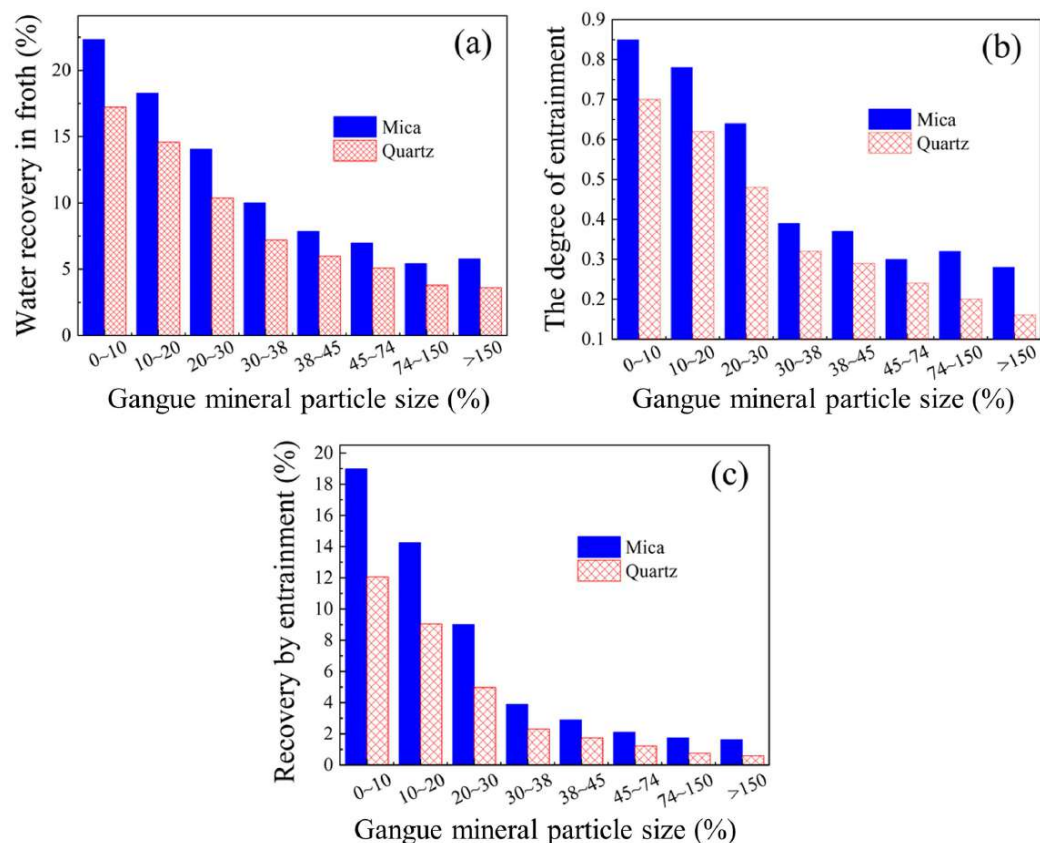


Figure 6. The effect of gangue particle size on its entrainment behavior: (a) the water recovery in froth; (b) the degree of entrainment; and (c) the recovery of gangue by entrainment.

The changed water recovery, therefore, substantially impacts the entrainment of gangue minerals. As shown in Figure 6b, the degree of entrainment (e_g) of both mica and quartz decreases from 0.85 and 0.70 to only 0.28 and 0.16, respectively, as the particle size increases from -10 to $+150$ μm . It is indicative that particle shape also contributes to the entrainment, as the e_g of quartz is always lower than that of mica under the same size fraction. Similar results have been reported by Neethling [33]. Theoretically, particle shape affects drag coefficients of particles and thus hinders the settling rates of particles within plateau borders. It is suggested that the constantly higher entrainment of mica particles was attributed to the much lower settling rate of flaky shape mica than that of granular quartz particles, as demonstrated in the SEM images in Figure 4. However, it is difficult to investigate the dependence of particle shape on gangue entrainment because it may be concealed by the also changed surface roughness and, more likely, by other more influencing factors such as particle size, reagent type and dosage, and hydrophobicity.

As a product of R_W and e_g , the recovery of gangue minerals by entrainment (R_M) shows a more substantial increase with the decrease in particle size, especially when the particle size is less than 30 μm , as shown in Figure 6c. Specifically, the R_M values of mica and quartz with a particle size of $+150$ μm are 1.62% and 0.58%, respectively, indicating that almost no entrainment occurred. Some studies [34–36] indicated that the recovery of $+150$ μm size particle in froth cannot be defined as entrainment but contributed by true flotation. In contrast, the R_M of mica and quartz with a particle size of -10 μm dramatically increased to 18.99% and 12.05%, respectively.

3.1.2. Pulp Density

Apart from particle size, pulp density, which describes the mass of mineral in unit volume of the flotation pulp, also dramatically influences gangue entrainment. Figure 7 shows the entrainment behavior of mica and quartz (-74 to 45 μm) as a function of pulp

density with 20 mg/L sec-octanol added. As shown in Figure 7a, the R_W rises with increasing pulp density; similarly, the R_W of quartz froth is constantly inferior to that of mica froth throughout the pulp density range. It is suggested that apart from setting efficiency, particle shape also affects water drainage between the particles. The water drainage efficiency between flaky mica particles is lower than that between granular quartz particles. Thus, the water recovery of mica froth is constantly higher than quartz [37]. Increasing the solid concentration is anticipated to raise the slurry viscosity, leading to a higher froth liquid content and, thus, water recovery in the froth. As a result, the degree of entrainment and recovery of gangue minerals by entrainment are also intensified at higher pulp densities. As shown in Figure 7b, the entrainment rate of mica increases from 0.31 to 0.42, and that of quartz ascends from 0.24 to 0.35 as the pulp density rises from 2% to 30%. Figure 7c shows that the R_M of mica and quartz are 1.25% and 0.89%, respectively, when the pulp density is 2%. As the pulp density increases to 30%, the e_g of mica and quartz reach 8.69% and 5.87%, respectively, which are 6.95 and 6.60 times higher than those at a pulp density of 2%.

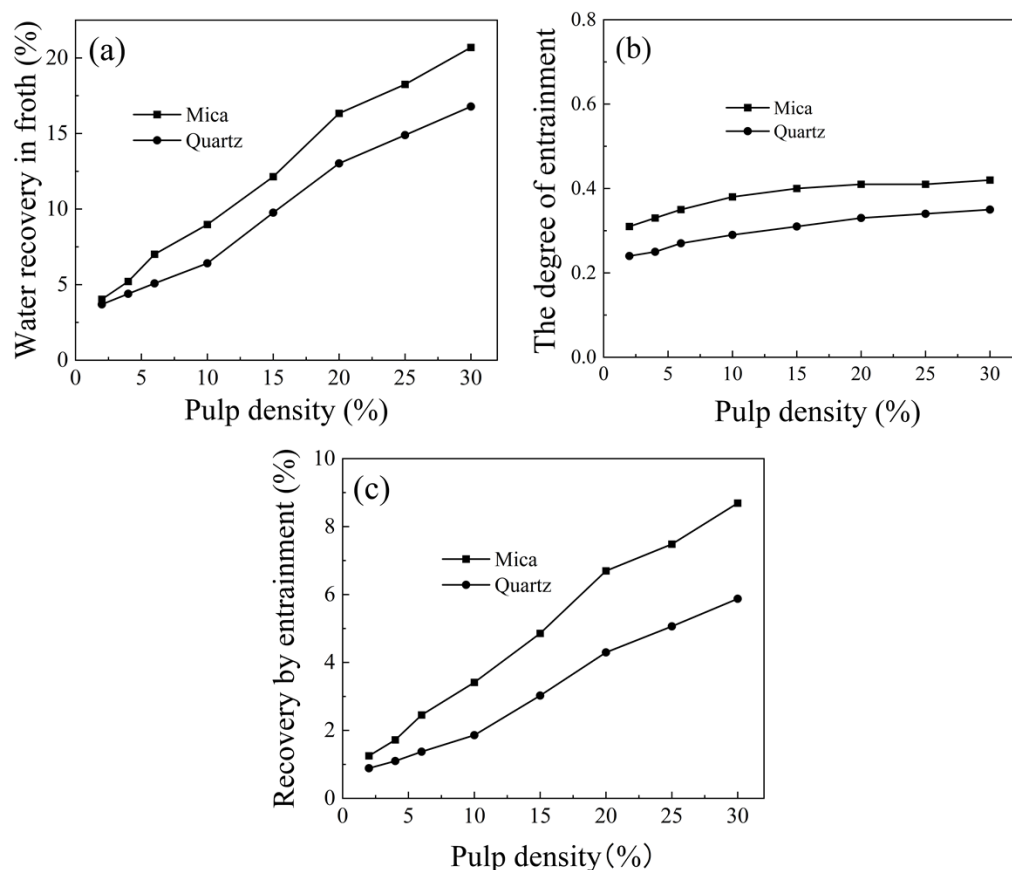


Figure 7. The effect of pulp density on (a) the water recovery in froth, (b) the degree of entrainment, and (c) the recovery of gangue minerals by entrainment.

3.1.3. Frother

Terpenic oil, MIBC, and sec-octanol are commonly used frothers in graphite flotation. Figure 8 compares the impact of these frothers on the entrainment behavior of mica and quartz. It can be seen from Figure 8a that the water recovery in froth for both gangues shows a similar upward trend as the frother increases; the R_W corresponding to MIBC is the largest, followed by sec-octanol and terpenic oil, under the same concentration conditions. A less noticeable increase in the degree of entrainment is observed in Figure 8b; the highest e_g is obtained with terpenic oil, which is followed by sec-octanol and MIBC. Similarly, in Figure 8c, the recovery of gangue minerals by entrainment also increases with increased

frother concentration. Notably, the R_M values corresponding to terpenic oil and MIBC are the highest for mica, while that for sec-octanol is much lower. For quartz, terpenic oil has the most significant impact on the R_M , which is followed by sec-octanol and MIBC.

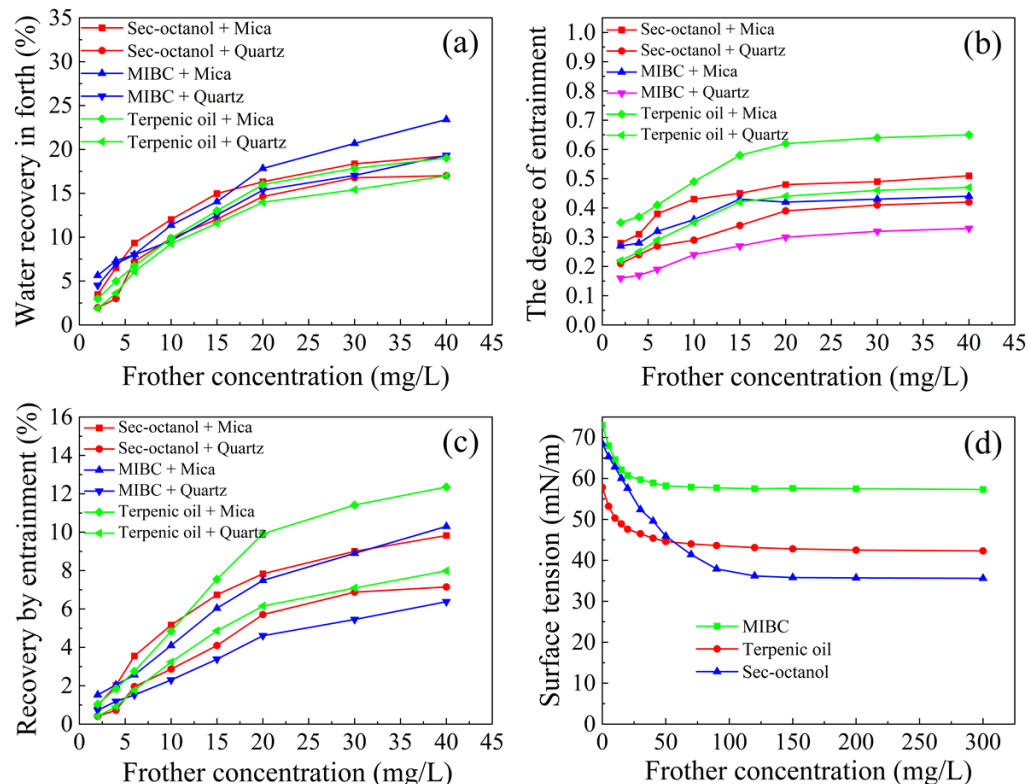


Figure 8. The effect of frother on the entrainment of gangue mineral flotation: (a) the water recovery in froth; (b) the degree of entrainment; (c) the recovery of gangue by entrainment; and (d) the surface tension of solutions with different frothers.

These surfactant-based frothers dramatically modify the surface tension of the solution and firmly shape the foaming performance and froth properties [38,39]. Figure 8d shows the surface tension of the solution as a function of the concentration of the three frothers. As the concentration of frother increases, the surface tension of the solution falls and reaches the equilibrium following the decreasing order: sec-octanol, terpenic oil, and MIBC. However, it should be noted that the surface tension of the solution in the frother range of 0–50 mg/L follows a different decreasing order of MIBC, sec-octanol, and terpenic oil. This is particularly important, since most flotation was carried out within a frother concentration no higher than 40 mg/L. The froth stability is inversely proportional to its surface tension [40]. The higher surface tension of MIBC solution renders a less stable froth, resulting in the highest water recovery. Consequently, the high water content in the froth enlarges the cross-sectional area of the froth platform, thus decreasing the entrainment of gangue minerals. On the contrary, the lowest surface tension of terpenic oil solution leads to the firmest froth stability, the lowest water recovery, and the highest gangue recovery by entrainment.

3.1.4. Collector

Oily hydrocarbon collectors are usually used for the enhanced flotation of hydrophobic non-polar minerals, such as graphite, talc, and coal. However, due to the insoluble nature of these collectors, they tend to exist as oil droplets in the flotation slurry [41,42] and form a thick oil film on the mineral surface. As a result, the dosage of these agents is demanding, 0.2 to 2 kg/t or more, which would worsen the froth stability and reduce the flotation selectivity. Excessive non-polar hydrocarbon oil molecules can squeeze the frother

molecules from the bubble surface or co-adsorb at the air–liquid interface, undermining the strength of the bubble surface and rendering bubble coalescence.

Kerosene and diesel are two commonly used collectors in graphite flotation. Studies have shown that kerosene with superior defoaming properties can stabilize the froth layer, ensure weightless foam volume, and increase foam product concentration. Our previous study [31] indicated that despite no interaction with gangue minerals, kerosene still strongly contributes to the collection of these gangue minerals in graphite flotation by changing the properties of flotation foam. Inspired by this, the effect of collector concentration on mica and quartz entrainment was investigated, and the results are shown in Figure 9.

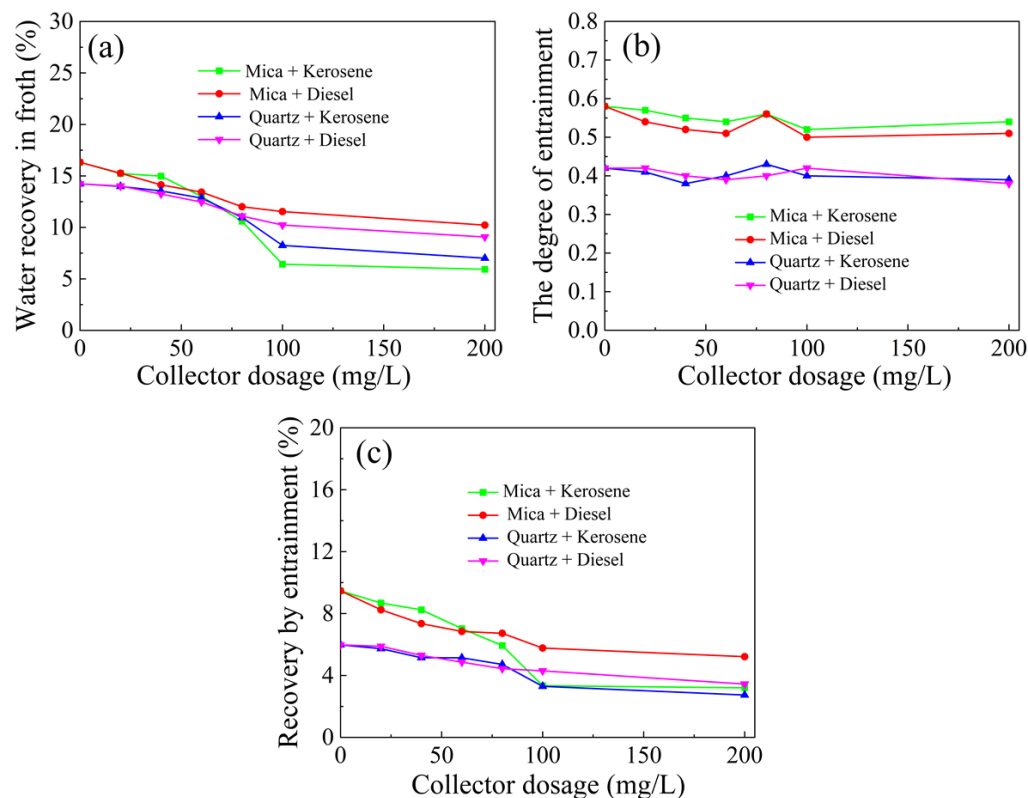


Figure 9. The effect of collectors on the entrainment of gangue mineral flotation: (a) the water recovery in froth; (b) the degree of entrainment; and (c) the recovery of gangue by entrainment.

It can be seen from Figure 9a that as the collector concentration increases, the water recovery in froth slightly decreases, with kerosene showing a more dramatic change than diesel. When the kerosene concentration increases from 0 to 200 mg/L, the R_W of mica and quartz froth decreases from 16.32% and 14.23% to 5.93% and 7.01%, respectively. Interestingly, there is no significant change in the e_g of either mica or quartz by collector concentration, as shown in Figure 9b. Nevertheless, the e_g of mica is always higher than that of quartz, regardless of the types of collectors used.

Moreover, the results in Figure 9c demonstrate that the R_M of gangue minerals gradually decreases as the collector concentration increases. In the absence of a collector, the R_M of mica and quartz are 9.47% and 5.98%, respectively. When diesel is used as a collector, the R_M values of mica and quartz decrease to 5.21% and 3.45%, respectively. A more substantial reduction is observed when kerosene is used, and the corresponding R_M values of mica and quartz fall to 3.20% and 2.73%, respectively. It is suggested that kerosene exhibits a superior “defoaming” feature to diesel; thus, it can alleviate the entrainment of gangue minerals. However, whether the “defoaming” of kerosene affects graphite flotation recovery remains uncertain.

3.2. The Effect of Flake Graphite on the Water Recovery in Froth

Hydrophobic minerals are believed to have a more significant influence on foam properties [43]; therefore, the size of graphite flakes must also impact the entrainment of gangue minerals. Figure 10 shows the effects of kerosene dosage, graphite particle size, and pulp density on the water recovery of froth products in graphite single mineral flotation.

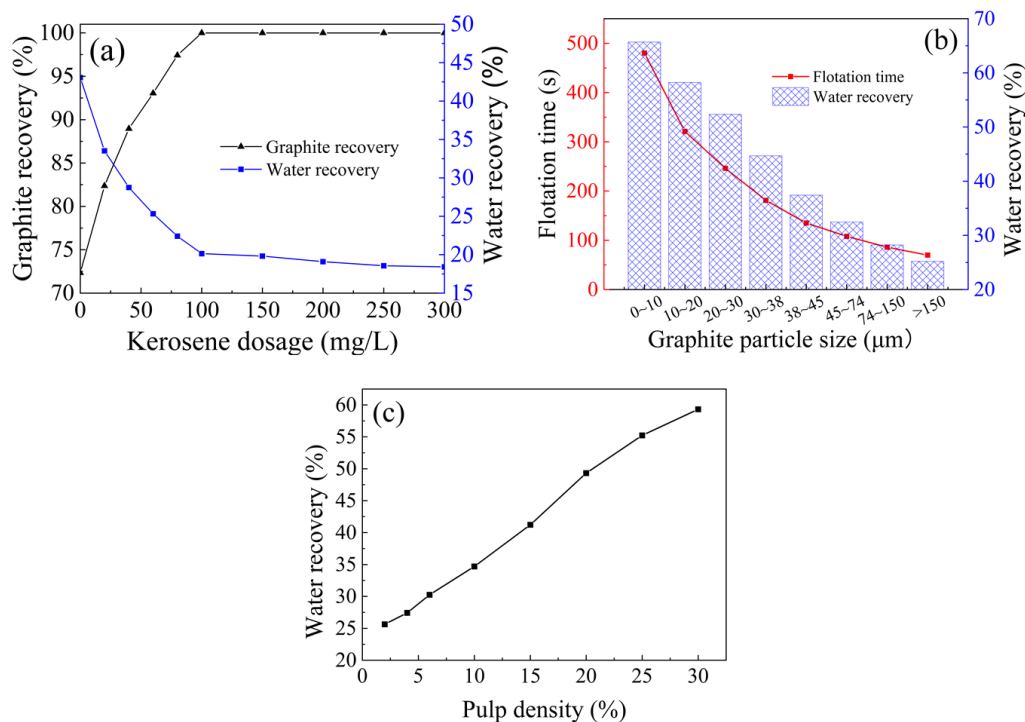


Figure 10. The effect of (a) kerosene dosage; (b) flake graphite particle size; and (c) pulp density on the water recovery in graphite concentrate.

Figure 10a demonstrates the effect of kerosene dosage on the water recovery in graphite concentrate. As the kerosene dosage increases, the flotation recovery of graphite significantly rises to nearly 100%. By contrast, the water recovery gradually declines from approximately 42% to 18%. Notably, as the graphite recovery reaches the maximum, the water recovery also decreases to the lowest level, implying that the influence of kerosene on froth water recovery is realized via enhanced collecting of graphite particles onto the froth phase. Figure 10b shows the water recovery of froth products from various graphite particle size fractions at 100 mg/L kerosene and 20 mg/L sec-octanol. There is a positive correlation between the water recovery and the flotation rate; the increased graphite flake size leads to a significant decrease in the water recovery and a dramatical reduction in flotation time. In addition, Figure 10c shows the effect of pulp density on the water recovery of the froth. It is evident that the water recovery increases considerably as the flotation slurry becomes denser, which might be attributed to the increased viscosity of the slurry [44,45], and thereby enhances the entrainment in the froth phase.

3.3. The Effect of Flake Graphite on the Entrainment Behavior of Gangue Mineral

3.3.1. Particle Size

Since graphite particles substantially impact the water recovery during flotation, it is not unreasonable to assume that the presence of graphite has a discernible effect on the entrainment of gangue. Therefore, the entrainment behavior of these gangue minerals was further investigated via mixed mineral flotation tests. The hydrophobic mineral particles can be irreversibly adsorbed at the gas/liquid interface during flotation, reducing the area of high-energy sites on the froth surface and, therefore, the energy of the entire froth system [46].

Figure 11 shows the effect of graphite flake size on the entrainment of mica and quartz in the mixed flotation with 100 mg/L kerosene, 20 mg/L sec-octanol, and 10% pulp density. As shown in Figure 11a,b, the water recovery shows a constant decrease with the increase in graphite particle size, which is similar to the results in single graphite flotation. It can be seen from Figure 11c,d that the smaller the graphite particle size, the higher the degree of gangue entrainment. The e_g of mica and quartz are 1.27 and 1.08, respectively, when the particle size of flake graphite is $-10 \mu\text{m}$, and that of mica or quartz is $-38 \mu\text{m}$. Some gangue minerals may enter the concentrate through entrapment [47,48], resulting in an e_g larger than 1. When the particle size of flake graphite and gangue minerals are $+150 \mu\text{m}$ and $+74 \mu\text{m}$, respectively, the e_g of mica and quartz are only 0.42 and 0.38, confirming the substantial influence of graphite particle size on gangue entrainment.

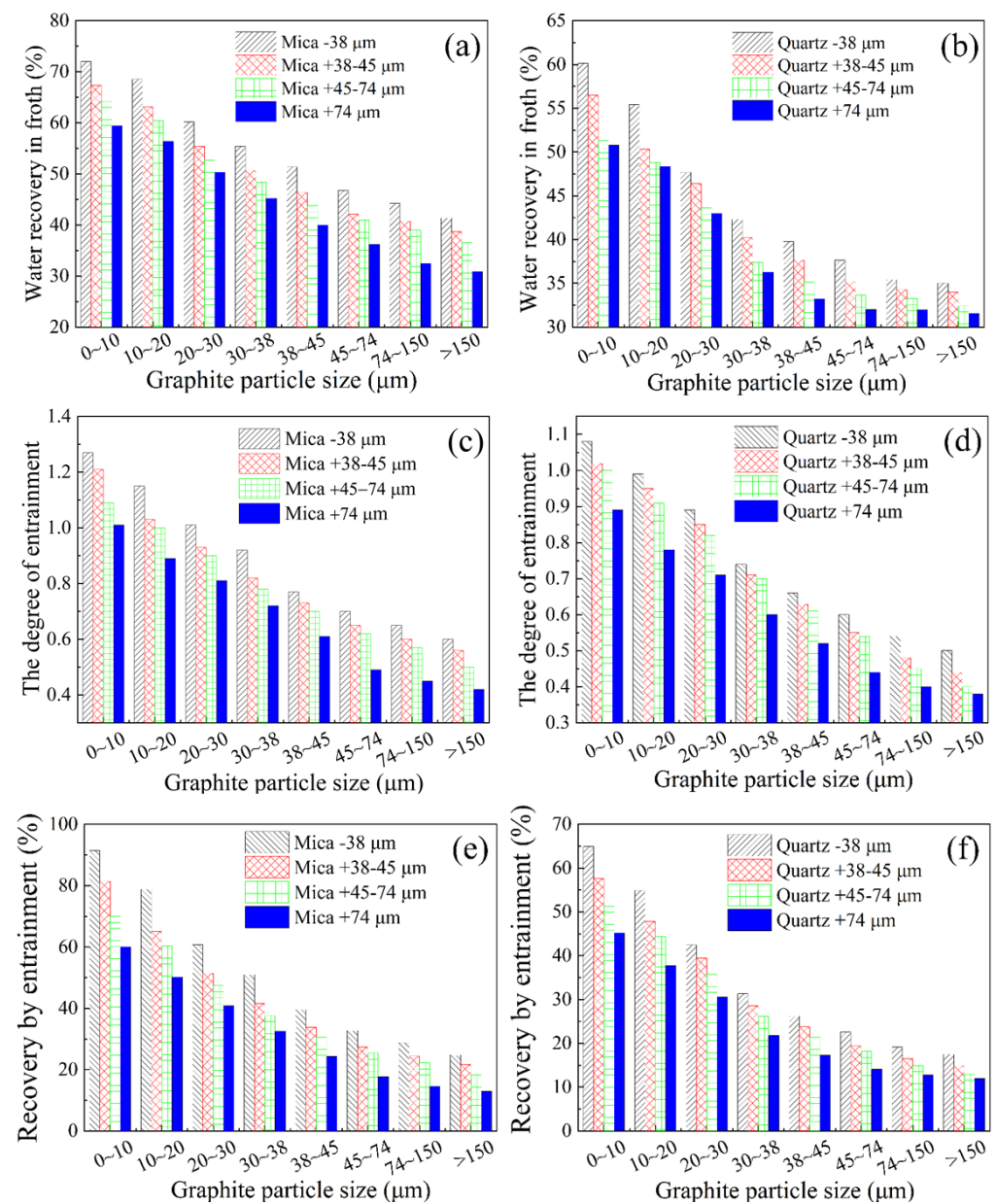


Figure 11. The effect of graphite particle size on the entrainment of gangue minerals in mixed flotation: (a,b) the water recovery in froth; (c,d) the degree of entrainment; and (e,f) the recovery of gangue by entrainment.

Figure 11e,f show that the recovery of quartz and mica by entrainment increases sharply as the particle size of flake graphite becomes finer. At a coarser graphite size of +150 μm and gangue size of +74 μm , the recovery of mica and quartz is only 12.96% and 11.99%, respectively. However, as flake graphite and gangue particle size decrease to $-10\ \mu\text{m}$ and $-38\ \mu\text{m}$, the recoveries of mica and quartz dramatically rise to 91.45% and 64.93%, respectively. Moreover, with the same graphite size of $-10\ \mu\text{m}$, the recovery of $-38\ \mu\text{m}$ mica is 91.45%, while that of +74 μm mica is only 60.04%, indicating that the finer the gangue mineral, the stronger the entrainment.

3.3.2. Pulp Density

Figure 12 shows the entrainment behavior of gangue minerals as a function of pulp density in the mixed flotation. As shown in Figure 12a, the water recovery in mixed mineral flotation positively correlates with the pulp density. Nevertheless, the water recovery of froth products in the presence of mica and quartz is higher than that of flake graphite single mineral flotation, indicating that the water brought into the concentrate by gangue minerals is more significant than that of flake graphite alone. Usually, the collection of graphite is via true flotation, while gangue minerals enter the concentrate mainly through entrainment. Therefore, the higher water recovery is primarily attributed to the strong entrainment of gangue minerals, and such water entrainment becomes more significant at higher pulp densities. As expected, the degree of entrainment of gangue minerals surges with the increase in pulp density. As shown in Figure 12b, the e_g values of mica and quartz in mixed mineral flotation are higher than 1, reaching 1.21 and 1.09, respectively, at the pulp density of 30%. Compared to the highest e_g of only 0.42 (Figure 7b) in the single gangue flotation, it is evident that the presence of hydrophobic flake graphite significantly intensified the entrainment of gangue minerals.

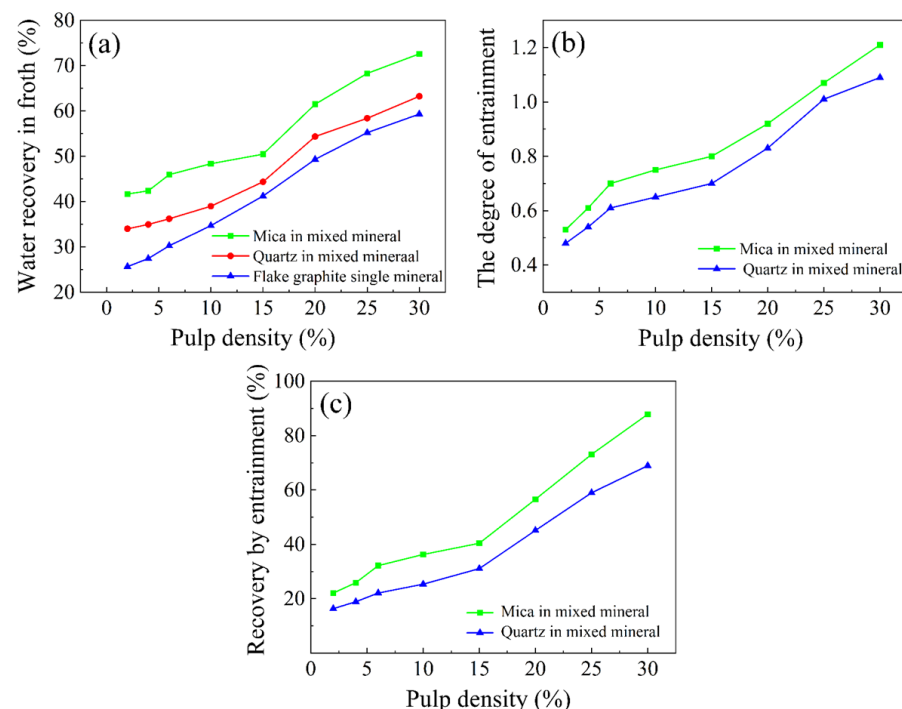


Figure 12. The effect of pulp density on the entrainment of gangue minerals in mixed flotation: (a) the water recovery in froth; (b) the degree of entrainment; and (c) the recovery of gangue by entrainment.

Compared with the single mineral flotation (Figure 7c), the recoveries of mica and quartz in Figure 12c have increased by nearly 80% and 60%, respectively. A similar observation was reported in Ata's research [29]. The entrainment of gangue minerals is closely related to the structure and characteristics of the froth. Hydrophobic flake graphite

in the mixed pulp reduces the probability of froth rupture and remarkably improves the froth stability. At the same time, the high pulp density improves the tried-and-true viscosity and stability of the froth, so more gangue minerals are entrained into the concentrate, leading to an increased recovery of gangue minerals by entrainment.

3.4. Flotation of Mixed Minerals of the Same Particle Size

In graphite beneficiation, the minerals are usually subjected to multiple grinding and milling processes. As a result, the flotation of actual graphite ores usually consists of similarly distributed graphite and gangue particles. Table 2 compares the flotation of mixed graphite and gangue minerals with the same particle size fractions of $-38\ \mu\text{m}$ and $-20\ \mu\text{m}$. The concentration of flotation pulp was 4%, and the collector and frother concentrations were 200 mg/L and 20 mg/L, respectively.

Table 2. Comparison of the flotation results of two artificial mixtures with the size fractions of $-38\ \mu\text{m}$ and $-20\ \mu\text{m}$.

Size Fraction of Mixtures	$-38\ \mu\text{m}$	$-20\ \mu\text{m}$
Yield of concentrate (%)	84.49	89.06
FC of concentrate (%)	78.82	74.78
Recovery of concentrate (%)	99.9	99.9
Water recovery in froth (%)	63.14	70.08
The degree of entrainment	0.85	0.96
Recovery of gangue by entrainment (%)	53.68	67.38
FC of mixtures (%)	66.67	66.67

It can be seen from Table 2 that the FC of the mixed minerals is 66.67%, which was considered to be the grade of “raw ore” in flotation. The FC content of final graphite concentrates just reached 78.82% ($-38\ \mu\text{m}$ size fraction) and 74.78% ($-20\ \mu\text{m}$ size fraction), respectively, indicating that plentiful gangue minerals entered the graphite concentrate through entrainment. In particular, the recovery of gangue minerals increased to 67.38% in the $-20\ \mu\text{m}$ mixtures compared to 53.68% in the $-38\ \mu\text{m}$ mixtures. Given the fully liberated nature between graphite and gangue minerals in the artificial mixtures, it is not unreasonable to assume more substantial gangue entrainment in actual graphite ore flotation, where a more complicated association between graphite and gangue minerals is expected.

4. Conclusions

The entrainment behavior of mica and quartz minerals in flake graphite flotation was systematically studied in this work. Our results indicated that particle size, pulp density, and flotation reagents all contribute to the entrainment of mica and quartz in graphite flotation by shaping froth properties.

Single flotation tests of gangue mineral revealed that the entrainment is more severe at finer particle size distributions. In addition, the pulp density strongly affects the water recovery in froth and the recovery of gangue minerals by entrainment but has no apparent influence on the degree of entrainment of gangue. The collector and frother change the stability of the froth phase. The superior froth stability is somehow detrimental to the flotation due to enhanced entrainment of gangue minerals. Compared to diesel, kerosene with better “defoaming” performance can reduce the entrainment of gangue minerals more effectively.

More significant gangue entrainment was observed in mixed flotation, indicating the substantial impact of hydrophobic graphite particles on the stability of the froth. Similar to the single mineral flotation, the flotation of homogeneously distributed mixtures confirmed that a finer particle size renders more severe gangue entrainment and thereby decreases the grade of final graphite concentrate. Therefore, future studies to minimize the entrainment in flake graphite flotation are proposed, such as optimization of the grinding process to avoid over-grinding and selective aggregation of fine particles to enlarge the particle size.

Author Contributions: Conceptualization, K.S.; Data curation, Z.M., Y.A. and W.L.; Formal analysis, Z.M., Y.A. and W.L.; Funding acquisition, Y.Q. (Yangshuai Qiu) and L.Z.; Investigation, Y.Q. (Yangshuai Qiu); Methodology, Z.M.; Resources, L.Z., Y.Q. (Yupeng Qian) and T.L.; Validation, K.S., Y.Q. (Yupeng Qian) and T.L.; Visualization, Y.A. and W.L.; Writing—original draft, Z.M.; Writing—review and editing, Y.Q. (Yangshuai Qiu) and K.S. All authors have read and agreed to the published version of the manuscript.

Funding: This work was supported by the China National Key R&D Program during the 14th Five-year Plan Period (Grant No. 2021YFC2902901) and the Key R&D Program of Hubei Province (Grant No. 2021BCA152).

Data Availability Statement: Not applicable.

Acknowledgments: The authors thank the above funding for their financial support for this project. The authors also thank the contributions of the reviewers for this manuscript.

Conflicts of Interest: The authors declare no conflict of interest.

References

1. Jara, A.D.; Betemariam, A.; Woldetinsae, G.; Kim, J.Y. Purification, application and current market trend of natural graphite: A review. *Int. J. Min. Sci. Technol.* **2019**, *29*, 671–689. [\[CrossRef\]](#)
2. Tamashauskyy, A.V. Graphite: A Multifunctional Additive for Paint and Coatings. *Am. Ceram. Soc. Bull.* **1998**, *77*, 102–104.
3. Crossley, P. Graphite—High-tech supply sharpens up. *Ind. Miner.* **2000**, *398*, 31–47.
4. Chelgani, S.C.; Rudolph, M.; Kratzsch, R.; Sandmann, D.; Gutzmer, J. A Review of Graphite Beneficiation Techniques. *Miner. Process. Extr. Metall. Rev.* **2016**, *37*, 58–68. [\[CrossRef\]](#)
5. Sun, K.K.; Qiu, Y.S.; Zhang, L.Y. Preserving Flake Size in an African Flake Graphite Ore Beneficiation Using a Modified Grinding and Pre-Screening Process. *Minerals* **2017**, *7*, 115. [\[CrossRef\]](#)
6. Wakamatsu, T.; Numata, Y. Flotation of graphite. *Miner. Eng.* **1991**, *4*, 975–982. [\[CrossRef\]](#)
7. Leja, J. *Surface Chemistry of Froth Flotation*; Springer: New York, NY, USA, 1982.
8. Jara, A.D.; Woldetinsae, G.; Betemariam, A.; Kim, J.Y. Mineralogical and petrographic analysis on the flake graphite ore from Saba Boru area in Ethiopia. *Int. J. Min. Sci. Technol.* **2020**, *30*, 715–721. [\[CrossRef\]](#)
9. Peng, W.; Qiu, Y.; Zhang, L.; Guan, J.; Song, S. Increasing the Fine Flaky Graphite Recovery in Flotation via a Combined Multiple Treatments Technique of Middlings. *Minerals* **2017**, *7*, 208. [\[CrossRef\]](#)
10. Peng, W.J.; Wang, C.; Hu, Y.; Song, S.X. Effect of droplet size of the emulsified kerosene on the floatation of amorphous graphite. *J. Dispers. Sci. Technol.* **2017**, *38*, 889–894. [\[CrossRef\]](#)
11. Wang, X.X.; Bu, X.N.; Ni, C.; Zhou, S.Q.; Yang, X.L.; Zhang, J.; Alheshibri, M.; Peng, Y.L.; Xie, G.Y. Effect of scrubbing medium particle size on scrubbing flotation performance and mineralogical characteristics of microcrystalline graphite. *Miner. Eng.* **2021**, *163*, 106766. [\[CrossRef\]](#)
12. Weng, X.Q.; Li, H.Q.; Song, S.X.; Liu, Y.Y. Reducing the Entrainment of Gangue Fines in Low Grade Microcrystalline Graphite Ore Flotation Using Multi-Stage Grinding-Flotation Process. *Minerals* **2017**, *7*, 38. [\[CrossRef\]](#)
13. Zhou, S.Q.; Wang, X.X.; Bu, X.N.; Shao, H.Z.; Hu, Y.; Alheshibri, M.; Li, B.; Ni, C.; Peng, Y.L.; Xie, G.Y. Effects of emulsified kerosene nanodroplets on the entrainment of gangue materials and selectivity index in aphanitic graphite flotation. *Miner. Eng.* **2020**, *158*, 106592. [\[CrossRef\]](#)
14. Bu, X.N.; Zhang, T.T.; Chen, Y.R.; Peng, Y.L.; Xie, G.Y.; Wu, E.D. Comparison of mechanical flotation cell and cyclonic microbubble flotation column in terms of separation performance for fine graphite. *Physicochem. Probl. Miner. Process.* **2018**, *54*, 732–740.
15. Bu, X.N.; Zhang, T.T.; Peng, Y.L.; Xie, G.Y.; Wu, E.D. Multi-Stage Flotation for the Removal of Ash from Fine Graphite Using Mechanical and Centrifugal Forces. *Minerals* **2018**, *8*, 15. [\[CrossRef\]](#)
16. Jin, M.G.; Xie, G.Y.; Xia, W.C.; Peng, Y.L. Flotation Optimization of Ultrafine Microcrystalline Graphite Using a Box-Behnken Design. *Int. J. Coal Prep. Utilization* **2018**, *38*, 281–289. [\[CrossRef\]](#)
17. Li, H.; Feng, Q.; Yang, S.; Ou, L.; Lu, Y. The entrainment behaviour of sericite in microcrystalline graphite flotation. *Int. J. Miner. Process.* **2014**, *127*, 1–9. [\[CrossRef\]](#)
18. Li, H.; Ou, L.; Feng, Q. The Recovery Mechanisms of Sericite in Microcrystalline Graphite Flotation. *Physicochem. Probl. Miner. Process.* **2015**, *51*, 387–400.
19. Ross, V.E. Flotation and entrainment of particles during batch flotation tests. *Miner. Eng.* **1990**, *3*, 245–256. [\[CrossRef\]](#)
20. Wang, L.; Peng, Y.; Runge, K.; Bradshaw, D. A review of entrainment: Mechanisms, contributing factors and modelling in flotation. *Miner. Eng.* **2015**, *70*, 77–91. [\[CrossRef\]](#)
21. Miettinen, T.; Ralston, J.; Fornasiero, D. The limits of fine particle flotation. *Miner. Eng.* **2010**, *23*, 420–437. [\[CrossRef\]](#)
22. Wang, L.; Peng, Y.; Runge, K. Entrainment in froth flotation: The degree of entrainment and its contributing factors. *Powder Technol.* **2016**, *288*, 202–211. [\[CrossRef\]](#)
23. Liang, L.; Tan, J.; Li, B.; Xie, G. Reducing quartz entrainment in fine coal flotation by polyaluminum chloride. *Fuel* **2019**, *235*, 150–157. [\[CrossRef\]](#)

24. Duarte, A.C.P.; Grano, S.R. Mechanism for the recovery of silicate gangue minerals in the flotation of ultrafine sphalerite. *Miner. Eng.* **2007**, *20*, 766–775. [[CrossRef](#)]
25. Gong, J.; Peng, Y.; Bouajila, A.; Ourriban, M.; Yeung, A.; Liu, Q. Reducing quartz gangue entrainment in sulphide ore flotation by high molecular weight polyethylene oxide. *Int. J. Miner. Process.* **2010**, *97*, 44–51. [[CrossRef](#)]
26. Silvester, E.J.; Heyes, G.W.; Bruckard, W.J.; Woodcock, J.T. The recovery of sericite in flotation concentrates. *Miner. Process. Extr. Metallurgy* **2011**, *120*, 10–14. [[CrossRef](#)]
27. Leistner, T.; Peuker, U.A.; Rudolph, M. How gangue particle size can affect the recovery of ultrafine and fine particles during froth flotation. *Miner. Eng.* **2017**, *109*, 1–9. [[CrossRef](#)]
28. Neethling, S.J.; Cilliers, J.J. The entrainment factor in froth flotation: Model for particle size and other operating parameter effects. *Int. J. Miner. Process.* **2009**, *93*, 141–148. [[CrossRef](#)]
29. Ata, S. Phenomena in the froth phase of flotation—A review. *Int. J. Miner. Process.* **2012**, *102–103*, 1–12. [[CrossRef](#)]
30. Kirjavainen, V.M. Review and analysis of factors controlling the mechanical flotation of gangue minerals. *Int. J. Miner. Process.* **1996**, *46*, 21–34. [[CrossRef](#)]
31. Xu, W.; Sun, K.; Qiu, Y.; Zhang, L.; Yang, L.; Wei, S.; Ding, D. Understanding the collection behavior of gangue minerals in fine flake graphite flotation. *Physicochem. Probl. Miner. Process.* **2022**, *58*, 101–112. [[CrossRef](#)]
32. Qiu, Y.S.; Zhang, L.Y.; Sun, K.K.; Li, Y.; Qian, Y.P. Reducing entrainment of sericite in fine flaky graphite flotation using polyaluminum chloride. *Physicochem. Probl. Miner. Process.* **2019**, *55*, 1108–1119.
33. Neethling, S.J.; Lee, H.T.; Cilliers, J.J. Simple relationships for predicting the recovery of liquid from flowing foams and froths. *Miner. Eng.* **2003**, *16*, 1123–1130. [[CrossRef](#)]
34. George, P.; Nguyen, A.V.; Jameson, G.J. Assessment of true flotation and entrainment in the flotation of submicron particles by fine bubbles. *Miner. Eng.* **2004**, *17*, 847–853. [[CrossRef](#)]
35. Cilek, E.C. The effect of hydrodynamic conditions on true flotation and entrainment in flotation of a complex sulphide ore. *Int. J. Miner. Process.* **2009**, *90*, 35–44. [[CrossRef](#)]
36. GÜler, T.; Akdemir, Ü. Statistical evaluation of flotation and entrainment behavior of an artificial ore. *Trans. Nonferrous Met. Soc. China* **2012**, *22*, 199–205. [[CrossRef](#)]
37. Xia, W. Role of particle shape in the floatability of mineral particle: An overview of recent advances. *Powder Technol.* **2017**, *317*, 104–116. [[CrossRef](#)]
38. Wang, H.; Li, J.; Wang, Z.; Wang, D.; Zhan, H. Experimental Investigation of the Mechanism of Foaming Agent Concentration Affecting Foam Stability. *J. Surfactants Detergents* **2017**, *20*, 1443–1451. [[CrossRef](#)]
39. Wang, H.; Wei, X.; Du, Y.; Wang, D. Effect of water-soluble polymers on the performance of dust-suppression foams: Wettability, surface viscosity and stability. *Colloids Surf. A Physicochem. Eng. Aspects* **2019**, *568*, 92–98. [[CrossRef](#)]
40. Ke, Y.; Shen, B.; Sun, H.; Liu, J.; Xu, X. Study on foaming of formulated solvent UDS and improving foaming control in acid natural gas sweetening process. *J. Nat. Gas Sci. Eng.* **2016**, *28*, 271–279. [[CrossRef](#)]
41. Xia, W.; Zhou, C.; Peng, Y. Improving flotation performance of intruded coal using heavy oil as a collector. *Energy Sources Part A Recovery Util. Environ. Effects* **2017**, *39*, 1124–1130. [[CrossRef](#)]
42. Xia, Y.; Yang, Z.; Zhang, R.; Xing, Y.; Gui, X. Performance of used lubricating oil as flotation collector for the recovery of clean low-rank coal. *Fuel* **2019**, *239*, 717–725. [[CrossRef](#)]
43. Rudolph, M.; Peuker, U.A. Hydrophobicity of Minerals Determined by Atomic Force Microscopy—A Tool for Flotation Research. *Chem. Ing. Technik* **2014**, *86*, 865–873. [[CrossRef](#)]
44. Hou, J.; Ma, X.; Fan, Y.; Dong, X.; Yao, S. Effect of particle properties on rheology of low-concentration coal suspensions. *Physicochem. Probl. Miner. Process.* **2020**, *56*, 984–995. [[CrossRef](#)]
45. Li, G.; Deng, L.; Cao, Y.; Wang, B.; Ran, J.; Zhang, H. Effect of sodium chloride on fine coal flotation and discussion based on froth stability and particle coagulation. *Int. J. Miner. Process.* **2017**, *169*, 47–52. [[CrossRef](#)]
46. Gonzenbach, U.T.; Studart, A.R.; Tervoort, E.; Gauckler, L.J. Stabilization of Foams with Inorganic Colloidal Particles. *Langmuir* **2006**, *22*, 10983–10988. [[CrossRef](#)]
47. Wang, B.; Peng, Y. The behaviour of mineral matter in fine coal flotation using saline water. *Fuel* **2013**, *109*, 309–315. [[CrossRef](#)]
48. Zheng, X.; Johnson, N.W.; Franzidis, J.P. Modelling of entrainment in industrial flotation cells: Water recovery and degree of entrainment. *Miner. Eng.* **2006**, *19*, 1191–1203. [[CrossRef](#)]